

Relaxation time for the alignment between the spin of a finite-mass quark/antiquark and the thermal vorticity in relativistic heavy-ion collisions

Alejandro Ayala^{a,b}, David de la Cruz^{a,c}, L. A. Hernández^{a,b,d}, Jordi Salinas^{*a}

^a*Instituto de Ciencias Nucleares, Universidad Nacional Autónoma de México, Apartado Postal 70-543, México Distrito Federal 04510, Mexico*

^b*Centre for Theoretical and Mathematical Physics, and Department of Physics, University of Cape Town, Rondebosch 7700, South Africa*

^c*Departamento de Física, Escuela Superior de Física y Matemáticas del Instituto Politécnico Nacional, Unidad Adolfo López Mateos, Edificio 9, 07738 Ciudad de México, México*

^d*Facultad de Ciencias de la Educación, Universidad Autónoma de Tlaxcala, Tlaxcala, 90000, Mexico.*

Abstract

We study the relaxation time required for the alignment between the spin of a finite-mass quark/antiquark and the thermal vorticity, at finite temperature and baryon chemical potential, in the context of relativistic heavy-ion collisions. The relaxation time is computed as the inverse of the total reaction rate that in turn is obtained from the imaginary part of the quark/antiquark self-energy. We model the interaction between spin and thermal vorticity within the medium by means of a vertex coupling quarks and thermal gluons that, for a uniform temperature, is proportional to the global angular velocity and inversely proportional to the temperature. We use realistic estimates for the angular velocities for different collision energies and show that the effect of the quark mass is to reduce the relaxation times as compared to the massless quark case. Using these relaxation times we estimate the intrinsic quark and antiquark polarizations produced by the thermal vorticity. We conclude by pointing out that, in spite of the former being larger than the latter, it is still possible to understand recent results from the STAR Beam Energy Scan when accounting for the fact that only a portion of quarks/antiquarks come from the denser and thus thermalized region in the collision.

Results from heavy-ion collisions experiments have contributed significantly to our understanding of the properties of strongly interacting matter at high temperature and density. In these reactions, two atomic nuclei collide at relativistic energies producing a deconfined state of hadronic matter, the so called quark-gluon plasma (QGP). Although many properties of this state have been revealed by means of a number of different probes, it is also fair to say that others still remain elusive at large. One of these has to do with the possibility to create a vortical fluid in peripheral collisions. Were this to be the case, the most promising way to elucidate its properties is by means of the alignment of particle spin to the global angular momentum, which in turn could be detected measuring a non-vanishing global particle polarization. This possibility has prompted the search for global polarization of hadrons, most notably of Λ and $\bar{\Lambda}$ [1, 2, 3, 4, 5, 6, 7, 8, 9, 10, 11, 12, 13, 14, 15, 16]. The STAR Beam Energy Scan (BES) program has measured the Λ and $\bar{\Lambda}$ global polarizations as functions of the collision energy [17, 18, 19] showing that as the latter decreases, the $\bar{\Lambda}$ polarization rises more steeply than the Λ polarization. This intriguing result motivates the search for a deeper understanding of the conditions for the relaxation between angular momentum

^{*}corresponding author: jordissm@ciencias.unam.mx

and spin degrees of freedom and of its dependence on the collision parameters such as energy, impact parameter, temperature, and quark chemical potential.

In a previous work [20], we have studied the relaxation time for spin and thermal vorticity alignment in a QGP at finite temperature T and quark chemical potential $\mu_q = \mu_B/3$, where μ_B is the baryon chemical potential. For these purposes, we resorted to the computation of the quark self-energy where the interaction with thermal gluons is mediated by a phenomenological vertex that couples the thermal vorticity to spin. To make matters simpler, we performed the calculation for massless quarks whose momentum was small compared to T and/or μ_q . In this work we remove such approximations and compute the relaxation time for massive quarks with arbitrary momentum. We show that the effect of accounting for the quark mass produces that the interaction rate is larger which in turn translates into a smaller relaxation time, as compared to the massless quark case. Other attempts to compute the relaxation time using different approaches have been reported in Refs. [21, 22, 23].

In order to present a self-contained discussion, we hereby spell out the ingredients needed for the computation, highlighting the new elements as compared to Ref. [20]. Recall that the *thermal vorticity* is defined as [24]

$$\bar{\omega}_{\mu\nu} = \frac{1}{2} (\partial_\nu \beta_\mu - \partial_\mu \beta_\nu), \quad (1)$$

where $\beta_\mu = u_\mu(x)/T(x)$, with $u_\mu(x)$ the local fluid four-velocity and $T(x)$ the local temperature. Thermal vorticity is produced in peripheral collisions where the colliding matter develops a global angular velocity $\vec{\omega} = \omega \hat{z}$, normal to the reaction plane, that for our purposes is chosen as the direction of the \hat{z} axis. The orbital angular momentum is due to the inhomogeneity of the matter density profile in the transverse plane [25]. For a constant angular velocity and uniform temperature, the magnitude of the thermal vorticity is given by ω/T .

Consider a QCD plasma in thermal equilibrium at temperature T and quark chemical potential μ_q . The interaction rate Γ of a quark with four-momentum $P = (p_0, \vec{p})$ can be expressed in terms of the quark self energy Σ as

$$\Gamma(p_0) = \tilde{f}(p_0 - \mu_q) \text{Tr} \{ \gamma^0 \text{Im} \Sigma \}, \quad (2)$$

with $\tilde{f}(p_0 - \mu_q)$ being the Fermi-Dirac distribution. The interaction between the thermal vorticity and the quark spin is modeled by means of an effective vertex

$$\lambda_a^\mu = g \frac{\sigma^{\alpha\beta}}{2} \bar{\omega}_{\alpha\beta} \gamma^\mu t_a, \quad (3)$$

where $\sigma^{\alpha\beta} = \frac{i}{2} [\gamma^\alpha, \gamma^\beta]$ is the quark spin operator and t_a are the color matrices in the fundamental representation. The one-loop contribution to Σ , depicted in Fig. 1, is given explicitly by

$$\Sigma = T \sum_n \int \frac{d^3 k}{(2\pi)^3} \lambda_a^\mu S(\not{P} - \not{K}) \lambda_b^{\nu*} G_{\mu\nu}^{ab}(K), \quad (4)$$

where S and *G are the quark and effective gluon propagators, respectively. The intermediate quark line is taken as a bare quark propagator such that the inverse of the interaction rate corresponds to the relaxation time for the spin and vorticity alignment for quarks that are originally not thermalized.

In a covariant gauge, the Hard Thermal Loop (HTL) approximation to the effective gluon propagator is given by

$$^*G_{\mu\nu}(K) = ^*\Delta_L(K) P_{L\mu\nu} + ^*\Delta_T(K) P_{T\mu\nu}, \quad (5)$$

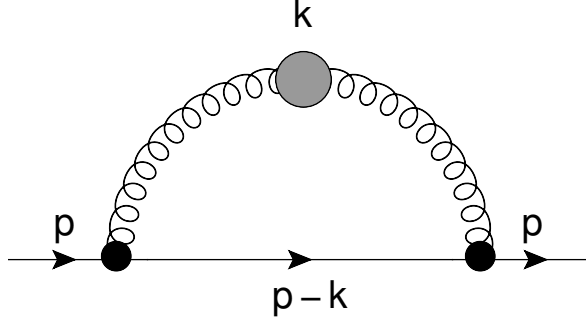


Figure 1: One-loop quark self-energy diagram that defines the kinematics. The gluon line with a blob represents the effective gluon propagator at finite density and temperature. The blobs on the quark-gluon vertices represent the effective coupling between the quark spin and the vorticity.

where $P_{L,T\mu\nu}$ are the polarization tensors for three dimensional longitudinal and transverse gluons, both of which are, of course, four-dimensionally transverse. The gluon propagator functions for longitudinal and transverse modes, ${}^*\Delta_{L,T}(K)$, are given by

$$\begin{aligned} {}^*\Delta_L(K)^{-1} &= K^2 + 2m^2 \frac{K^2}{k^2} \left[1 - \left(\frac{i\omega_n}{k} \right) Q_0 \left(\frac{i\omega_n}{k} \right) \right], \\ {}^*\Delta_T(K)^{-1} &= -K^2 - m^2 \left(\frac{i\omega_n}{k} \right) \left\{ \left[1 - \left(\frac{i\omega_n}{k} \right)^2 \right] Q_0 \left(\frac{i\omega_n}{k} \right) + \left(\frac{i\omega_n}{k} \right) \right\}, \end{aligned} \quad (6)$$

where

$$Q_0(x) = \frac{1}{2} \ln \frac{x+1}{x-1}, \quad (7)$$

and m is the gluon thermal mass given by

$$m^2 = \frac{1}{6} g^2 C_A T^2 + \frac{1}{12} g^2 C_F \left(T^2 + \frac{3}{\pi^2} \mu^2 \right), \quad (8)$$

where $C_A = 3$ and $C_F = 4/3$ are the Casimir factors for the adjoint and fundamental representations of $SU(3)$, respectively.

The sum over Matsubara frequencies involves products of the propagator functions for longitudinal and transverse gluons ${}^*\Delta_{L,T}$ and the Matsubara propagator for the bare quark $\tilde{\Delta}_F$, such that the term that depends on the summation index can be expressed as

$$S_{L,T} = T \sum_n {}^*\Delta_{L,T}(i\omega_n) \tilde{\Delta}_F(i(\omega_m - \omega_n)). \quad (9)$$

This sum is more straightforward evaluated introducing the spectral densities $\rho_{L,T}$ and $\tilde{\rho}$ for the gluon and fermion propagators, respectively. The imaginary part of S_i , $i = L, T$, can thus be written as

$$\text{Im } S_i = \pi \left(e^{(p_0 - \mu_q)/T} + 1 \right) \int_{-\infty}^{\infty} \frac{dk_0}{2\pi} \int_{-\infty}^{\infty} \frac{dp'_0}{2\pi} f(k_0) \tilde{f}(p'_0 - \mu) \delta(p_0 - k_0 - p'_0) \rho_i(k_0) \tilde{\rho}(p'_0), \quad (10)$$

where $f(k_0)$ is the Bose-Einstein distribution. The spectral densities $\rho_{L,T}(k_0, k)$ are obtained from the imaginary part of ${}^*\Delta_{L,T}(i\omega_n, k)$ after the analytic continuation $i\omega_n \rightarrow k_0 + i\epsilon$ and contain the discontinuities of the gluon propagator across the real k_0 -axis. Their support depends on the ratio $x = k_0/k$. For $|x| > 1$, $\rho_{L,T}$ have support on

the (time-like) quasiparticle poles. For $|x| < 1$ their support coincides with the branch cut of $Q_0(x)$. On the other hand, the spectral density corresponding to a bare quark is given by

$$\tilde{\rho}(p'_0) = 2\pi\epsilon(p'_0)\delta(p_0'^2 - E_p^2), \quad (11)$$

where $E_p^2 = (p - k)^2 + m_q^2$ with m_q the quark mass. The kinematical restriction that Eq. (11) imposes on Eq. (10) limit the integration over gluon energies to the space-like region, namely, $|x| < 1$. Therefore, the parts of the gluon spectral densities that contribute to the interaction rate are given by

$$\begin{aligned} \rho_L(k_0, k) &= \frac{x}{1 - x^2} \frac{2\pi m^2 \theta(k^2 - k_0^2)}{[k^2 + 2m^2(1 - (x/2)\ln|(1+x)/(1-x)|)]^2 + [\pi m^2 x]^2} \\ \rho_T(k_0, k) &= \frac{\pi m^2 x(1 - x^2)\theta(k^2 - k_0^2)}{[k^2(1 - x^2) + m^2(x^2 + (x/2)(1 - x^2)\ln|(1+x)/(1-x)|)]^2 + [(\pi/2)m^2 x(1 - x^2)]^2}. \end{aligned} \quad (12)$$

Collecting all the ingredients, the interaction rate for a massive quark with energy p_0 to align its spin with the thermal vorticity is given by

$$\Gamma(p_0) = \frac{\alpha_s}{4\pi} \left(\frac{\omega}{T}\right)^2 \frac{C_F}{\sqrt{p_0^2 - m_q^2}} \int_0^\infty dk k \int_{\mathcal{R}} dk_0 [1 + f(k_0)] \tilde{f}(p_0 + k_0 - \mu_q) \sum_{i=L,T} C_i(p_0, k_0, k) \rho_i(k_0, k), \quad (13)$$

where \mathcal{R} represents the region $\sqrt{(\sqrt{p_0^2 - m_q^2} - k)^2 + m_q^2} - p_0 \leq k_0 \leq \sqrt{(\sqrt{p_0^2 - m_q^2} + k)^2 + m_q^2} - p_0$. The polarization coefficients $C_{L,T}$ come from the contraction of the polarization tensors $P_{L,T\mu\nu}$ with the trace of the factors involving Dirac gamma matrices from the self-energy. After implementing the kinematical restrictions for the allowed values of the angle between the quark and gluon momenta, these functions are found to be

$$\begin{aligned} C_T(p_0, k_0, k) &= 8(p_0 + k_0) \left(\frac{k^2 - 2k_0 p_0 - k_0^2}{2k\sqrt{p_0^2 - m_q^2}} \right)^2 \\ C_L(p_0, k_0, k) &= -8(p_0 + k_0) \left[\left(\frac{k^2 - 2k_0 p_0 - k_0^2}{2k\sqrt{p_0^2 - m_q^2}} \right)^2 - \frac{1}{2} \right] - 8 \frac{p_0 k^2}{k_0^2 - k^2} \left(\frac{k^2 - 2k_0 p_0 - k_0^2}{2k\sqrt{p_0^2 - m_q^2}} \right)^2. \end{aligned} \quad (14)$$

This result should be contrasted with Eq. (14) of Ref. [20], which was computed for the massless and small quark momentum limit.

The total interaction rate is obtained by integrating Eq. (13) over the available phase space

$$\Gamma = V \int \frac{d^3 p}{(2\pi)^3} \Gamma(p_0), \quad (15)$$

where V is the volume of the overlap region in the collision. Recall that, for the collision of symmetric systems of nuclei with radii R and a given impact parameter b , V is given by

$$V = \frac{\pi}{3} (4R + b)(R - b/2)^2. \quad (16)$$

We use the findings of Ref. [26] for the estimate of the angular velocity ω produced in the collisions at a given energy and impact parameter. From the expression for Γ in Eq. (15), we study the parametric dependence of the relaxation time for spin and vorticity alignment, defined as

$$\tau \equiv 1/\Gamma. \quad (17)$$

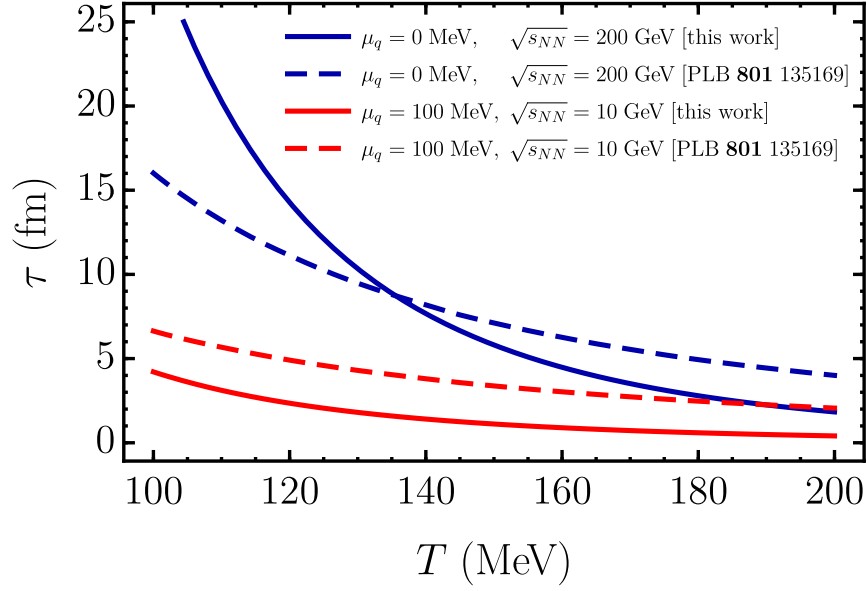


Figure 2: Relaxation time τ for quarks as a function of temperature T for semicentral collisions at an impact parameter $b = 10$ fm. In dashed lines, massless quarks [20] for $\sqrt{s_{NN}} = 10, 200$ GeV with $\omega \simeq 0.12, 0.10$ fm $^{-1}$, respectively. In solid lines, massive quarks for $\sqrt{s_{NN}} = 10, 200$ GeV with $\omega \simeq 0.06, 0.04$ fm $^{-1}$, respectively, using the findings of Ref. [26].

Figure 2 shows the temperature dependence of the relaxation time for quarks, for two different collision energies and quark chemical potentials at an impact parameter $b = 10$ fm, using for the quark mass $m_q = 100$ MeV,

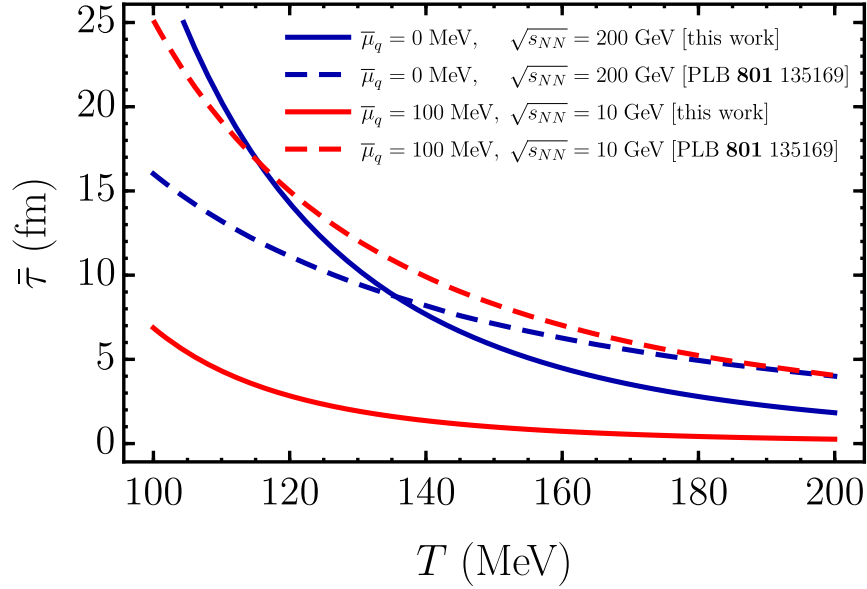


Figure 3: Relaxation time $\bar{\tau}$ for antiquarks as a function of temperature T for semicentral collisions at an impact parameter $b = 10$ fm. In dashed lines, massless quarks [20] for $\sqrt{s_{NN}} = 10, 200$ GeV with $\omega \simeq 0.12, 0.10$ fm $^{-1}$, respectively. In solid lines, massive quarks for $\sqrt{s_{NN}} = 10, 200$ GeV with $\omega \simeq 0.06, 0.04$ fm $^{-1}$, respectively, using the findings of Ref. [26].

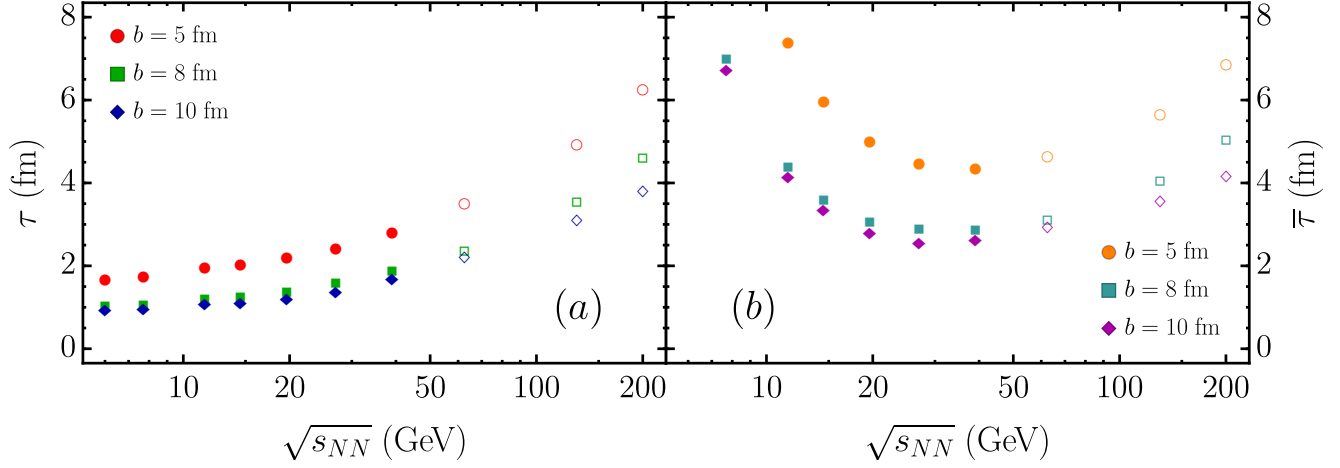


Figure 4: (a) Relaxation time τ for quarks as a function of $\sqrt{s_{NN}}$ for semicentral collisions at impact parameters $b = 5, 8, 10$ fm. (b) Relaxation time $\bar{\tau}$ for antiquarks as a function of $\sqrt{s_{NN}}$ for semicentral collisions at impact parameters $b = 5, 8, 10$ fm. For both, we used the findings of Ref. [26].

corresponding to the mass of the strange quark. Notice that $\tau \lesssim 5$ fm for the temperature range $150 \text{ MeV} < T < 200 \text{ MeV}$, where the phase transition is expected. In this temperature range, the relaxation times are smaller than the ones found in Ref. [20]. This may seem counter-intuitive given that a finite quark mass reduces the available phase space. However, notice that the new terms in Eq. (14) as compared to Eq. (14) of Ref. [20], compensate this reduction and contribute significantly to a higher interaction rate.

Figure 3 shows the temperature dependence of the relaxation time for antiquarks, for two different collision energies and chemical potentials at an impact parameter $b = 10$ fm. Again, we use for the antiquark mass $m_q = 100$ MeV, corresponding to the mass of the strange antiquark. The relaxation times for antiquarks for the temperature range $150 \text{ MeV} < T < 200 \text{ MeV}$ satisfy $\bar{\tau} \lesssim 5$ fm and are also smaller than the corresponding relaxation times found in Ref. [20].

Figure 4 shows the relaxation time (a) τ for quarks and (b) $\bar{\tau}$ for antiquarks as functions of $\sqrt{s_{NN}}$ for semicentral collisions at impact parameters $b = 5, 8, 10$ fm. The relation between the temperature and baryon chemical potential at freeze-out corresponding to maximum baryon density for each collision energy is obtained from the results of Ref. [27] such that

$$\begin{aligned} T(\mu_B) &= 166 - 139\mu_B^2 - 53\mu_B^4, \\ \mu_B(\sqrt{s_{NN}}) &= \frac{1308}{1000 + 0.273\sqrt{s_{NN}}}, \end{aligned} \quad (18)$$

where μ_B and T are given in MeV. For the estimate of the angular velocities corresponding to a given collision energy, we have used the findings of Ref. [26]. The open symbols correspond to extrapolated values for these angular velocities. Notice that the relaxation times for quarks show a monotonic growth as a function of the collision energy. In contrast, the corresponding relaxation times for antiquarks have a minimum for collision energies in the range $30 \text{ GeV} \lesssim \sqrt{s_{NN}} \lesssim 50 \text{ GeV}$.

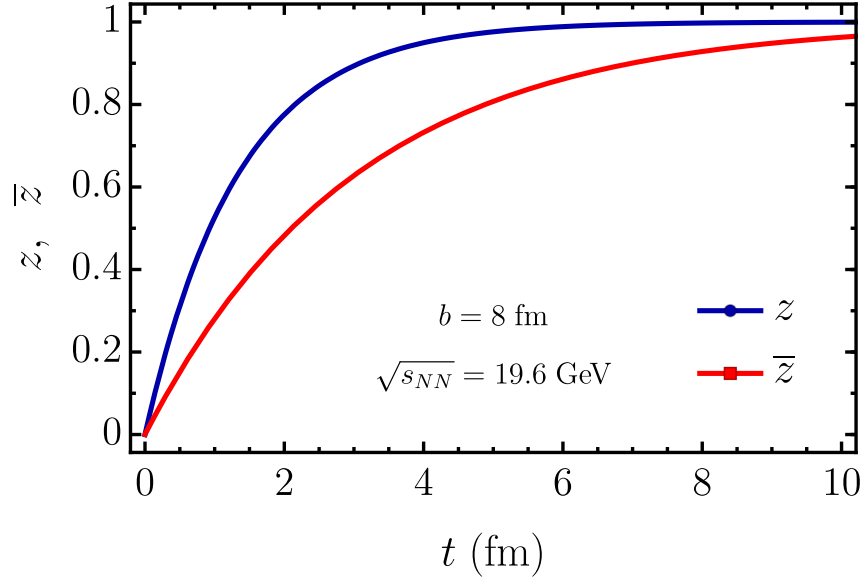


Figure 5: Intrinsic global polarization for quarks (z) and antiquarks (\bar{z}) as functions of time t for semicentral collisions at an impact parameter $b = 8$ fm for $\sqrt{s_{NN}} = 19.6$ GeV. Notice that $\bar{z} < z$, however, both intrinsic polarizations tend to 1 for $t \simeq 10$ fm.

Figure 5 shows the *intrinsic* global polarization [28] for quarks (z) and antiquarks (\bar{z}), given by

$$\begin{aligned} z &= 1 - e^{-t/\tau} \\ \bar{z} &= 1 - e^{-t/\bar{\tau}}, \end{aligned} \quad (19)$$

as functions of time t for semicentral collisions at an impact parameter $b = 8$ fm, for $\sqrt{s_{NN}} = 19.6$ GeV. Notice that $\bar{z} < z$, however, both intrinsic polarizations tend to 1 for $t \simeq 10$ fm. From this figure, we also notice that, even if the QGP phase lasts for less than 10 fm, a finite intrinsic global polarization, both for quarks and antiquarks, can still be expected.

When the intrinsic global polarization of strange quarks and antiquarks is preserved during the hadronization process, one might expect that these polarizations directly translate into the corresponding Λ and $\bar{\Lambda}$ polarizations. This would in turn imply that the former should be expected to be larger than the latter, as opposed to the findings of Ref. [18]. A hint that this is not necessarily the case has been recently put forward in Ref. [29] where the source of Λ s and $\bar{\Lambda}$ s in the reaction zone is modelled as composed of a high-density core and a less dense corona. Although both regions partake of the vortical motion, Λ s and $\bar{\Lambda}$ s coming from one or the other could show different polarization properties as their origins are different: in the core they come mainly from QGP induced processes, whereas in the corona they come from $n + n$ processes. When this fact is combined with a larger abundance of Λ s as compared to $\bar{\Lambda}$ s in the corona region together with a smaller number of Λ s coming from the core as compared to those coming from the corona –which happens for semi-central to peripheral collisions– an amplification effect for the $\bar{\Lambda}$ polarization can occur. This is more prominent for small collision energies. An explicit calculation of the consequences of this interplay between core and corona for Λ and $\bar{\Lambda}$ production is currently under way and will be reported elsewhere.

Acknowledgements

The authors acknowledge useful conversations with S. Hernández during the genesis of this work. Support has been received by UNAM-DGAPA-PAPIIT grant number IG100219. L. A. H. acknowledges support from a PAPIIT-DGAPA-UNAM fellowship.

References

- [1] F. Becattini, I. Karpenko, M. A. Lisa, I. Upsal, S. A. Voloshin, Global hyperon polarization at local thermodynamic equilibrium with vorticity, magnetic field, and feed-down, *Phys. Rev. C* **95** (2017) 113. <https://doi.org/10.1103/PhysRevC.95.054902>
- [2] Y. Xie, R. C. Glastad and L. P. Csernai, Λ polarization in an exact rotating and expanding fluid dynamical model for peripheral heavy ion reactions, *Phys. Rev. C* **92** (2015) 064901. <https://doi.org/10.1103/PhysRevC.92.064901>
- [3] A. Sorin and O. Teryaev, P-odd effects in heavy ion collisions at NICA, *Nucl. Part. Phys. Proc.* **273-275** (2016) 2587-2589. <https://doi.org/10.1016/j.nuclphysbps.2015.09.468>
- [4] A. Sorin and O. Teryaev, Axial anomaly and energy dependence of hyperon polarization in Heavy-Ion Collisions, *Phys. Rev. C* **95** (2017) 011902. <https://doi.org/10.1103/PhysRevC.95.011902>
- [5] Y. L. Xie, M. Bleicher, H. Stöcker, D. J. Wang, and L. P. Csernai, Λ polarization in peripheral collisions at moderate relativistic energies, *Phys. Rev. C* **94** (2016) 054907. <https://doi.org/10.1103/PhysRevC.94.054907>
- [6] H. Li, L.-G. Pang, Q. Wang and X.-L. Xia, Global Λ polarization in heavy-ion collisions from a transport model, *Phys. Rev. C* **96** (2017) 054908. <https://doi.org/10.1103/PhysRevC.96.054908>
- [7] Y. Sun and C. M. Ko, Λ hyperon polarization in relativistic heavy ion collisions from a chiral kinetic approach, *Phys. Rev. C* **96** (2017) 024906. <https://doi.org/10.1103/PhysRevC.96.024906>
- [8] Z.-Z. Han and J. Xu, Investigating different Λ and $\bar{\Lambda}$ polarizations in relativistic heavy-ion collisions, *Phys. Lett. B* **786** (2018) 255-259. <https://doi.org/10.1016/j.physletb.2018.10.001>
- [9] X.-L. Xia, H. Li, Z.-B. Tang and Q. Wang, Probing vorticity structure in heavy-ion collisions by local Λ polarization, *Phys. Rev. C* **98** (2018) 024905. <https://doi.org/10.1103/PhysRevC.98.024905>
- [10] M. Baznat, K. Gudima, A. Sorin and O. Teryaev, Hyperon polarization in heavy-ion collisions and holographic gravitational anomaly, *Phys. Rev. C* **97** (2018) 041902. <https://doi.org/10.1103/PhysRevC.97.041902>
- [11] I. Karpenko and F. Becattini, Lambda polarization in heavy ion collisions: from RHIC BES to LHC energies, *Nucl. Phys. A* **982** (2019) 519-522. <https://doi.org/10.1016/j.nuclphysa.2018.10.067>
- [12] D. Suvarieva, K. Gudima and A. Zinchenko, A Monte Carlo Study of Lambda Hyperon Polarization at BM@N, *Phys. Part. Nucl. Lett.* **15** (2018) 182-188. <https://doi.org/10.1134/S1547477118020115>

- [13] E. E. Kolomeitsev, V. D. Toneev and V. Voronyuk, Vorticity and hyperon polarization at energies available at JINR Nuclotron-based Ion Collider fAcility, *Phys. Rev. C* **97** (2018) 064902. <https://doi.org/10.1103/PhysRevC.97.064902>
- [14] Y. Xie, D. Wang and L. P. Csernai, Fluid Dynamics Study of the Λ Polarization for Au+Au Collisions at $\sqrt{s_{NN}} = 200$ GeV, *Eur. Phys. J. C* **80** (2020) 39. <https://doi.org/10.1140/epjc/s10052-019-7576-8>
- [15] Y. Guo, S. Shi, S. Feng and J. Liao, Magnetic Field Induced Polarization Difference between Hyperons and Anti-hyperons, *Phys. Lett. B* **798** (2019) 134929. <https://doi.org/10.1016/j.physletb.2019.134929>
- [16] H.-B. Li, X.-X. Ma, Polarization difference between hyperons and antihyperons induced by an external magnetic field, *Phys. Rev. D* **100** (2019) 076007. <https://doi.org/10.1103/PhysRevD.100.076007>
- [17] B. I. Abelev et al., STAR Collaboration, Global polarization measurement in Au+Au collisions, *Phys. Rev. C* **76** (2007) 024915. <https://doi.org/10.1103/PhysRevC.76.024915>, Erratum: *Phys. Rev. C* **95** (2017) 039906.
- [18] L. Adamczyk et al., STAR Collaboration, Global Λ hyperon polarization in nuclear collisions, *Nature* **548** (2017) 6265. <https://doi.org/10.1038/nature23004>.
- [19] J. Adam et al., STAR Collaboration, Global polarization of Λ hyperons in Au + Au collisions at $\sqrt{s_{NN}} = 200$ GeV, *Phys. Rev. C* **98** (2018) 014910. <https://doi.org/10.1103/PhysRevC.98.014910>.
- [20] A. Ayala, D. de la Cruz, S. Hernandez-Ortiz, L. A. Hernandez, J. Salinas, Relaxation time for quark spin and thermal vorticity alignment in heavy-ion collisions, *Phys. Lett. B* **801** (2020) 135169. <https://doi.org/10.1016/j.physletb.2019.135169>.
- [21] J. I. Kapusta, E. Rrapaj, S. Rudaz, Relaxation time for strange quark spin in rotating quark-gluon plasma, *Phys. Rev. C* **101** (2020) 024907. <https://doi.org/10.1103/physrevc.101.024907>.
- [22] S.Y.F. Liu, Y. Sun, C.M. Ko, Local spin polarizations in relativistic heavy ion collisions (2020). <http://arxiv.org/abs/2002.11752>.
- [23] S. Shi, C. Gale, S. Jeon, From Chiral Kinetic Theory To Spin Hydrodynamics (2020). <http://arxiv.org/abs/2002.01911>.
- [24] F. Becattini, G. Inghirami, V. Rolando, A. Beraudo, L. Del Zanna, A. De Pace, M. Nardi, G. Pagliara, V. Chandra, A study of vorticity formation in high energy nuclear collisions, *Eur. Phys. J. C* **75** (2015) 406. <https://doi.org/10.1140/epjc/s10052-015-3624-1>.
- [25] F. Becattini, F. Piccinini, J. Rizzo, Angular momentum conservation in heavy ion collisions at very high energy, *Phys. Rev. C* **77** (2008) 024906. <https://doi.org/10.1103/PhysRevC.77.024906>.
- [26] X.-G. Deng, X.-G. Huang, Y.-G. Ma, S. Zhang, Vorticity in low-energy heavy-ion collisions (2020). <http://arxiv.org/abs/2001.01371>.

- [27] J. Cleymans, H. Oeschler, K. Redlich, S. Wheaton, Comparison of chemical freeze-out criteria in heavy-ion collisions, Phys. Rev. C **73** (2006) 034905. <https://doi.org/10.1103/PhysRevC.73.034905>.
- [28] A. Ayala, Quark spin thermal vorticity alignment and the Λ , $\bar{\Lambda}$ polarization in heavy-ion collisions, 36th Winter Workshop on Nuclear Dynamics, Puerto Vallarta, Mexico, March 2020. <https://indico.cern.ch/event/841247/contributions/3740432/attachments/1998415/3334657/Ayala.pdf>.
- [29] I. Maldonado, Two-component source to explain Λ and $\bar{\Lambda}$ global polarization in non-central heavy-ion collisions, 36th Winter Workshop on Nuclear Dynamics, Puerto Vallarta, Mexico, March 2020. https://indico.cern.ch/event/841247/contributions/3740473/attachments/1999852/3337750/WWND2020_global_polarization.pdf